Biosensors and Bioelectronics 109 (2018) 190–196

Contents lists available at ScienceDirect

Biosensors and Bioelectronics

journal homepage: www.elsevier.com/locate/bios

Ultrasensitive photoelectrochemical biosensor for the detection of HTLV-I DNA: A cascade signal amplification strategy integrating λ-exonuclease aided target recycling with hybridization chain reaction and enzyme catalysis

Xiao-Mei Shi[a,c,1], Gao-Chao Fan[b,c,1], Xueying Tang[a], Qingming Shen[a,*], Jun-Jie Zhu[c,*]

[a] Key Laboratory for Organic Electronics and Information Displays & Jiangsu Key Laboratory for Biosensors, Institute of Advanced Materials (IAM), Jiangsu National Synergetic Innovation Center for Advanced Materials (SICAM), Nanjing University of Posts & Telecommunications, Nanjing 210023, PR China
[b] Key Laboratory of Sensor Analysis of Tumor Marker of Education Ministry, College of Chemistry and Molecular Engineering, Qingdao University of Science and Technology, Qingdao 266042, PR China
[c] State Key Laboratory of Analytical Chemistry for Life Science, School of Chemistry and Chemical Engineering, Nanjing University, Nanjing 210093, PR China

ARTICLE INFO

Keywords:
Photoelectrochemistry
DNA sensor
HTLV-I
Hybridization chain reaction
Signal amplification

ABSTRACT

Sensitive and specific detection of DNA is of great significance for clinical diagnosis. In this paper, an effective cascade signal amplification strategy was introduced into photoelectrochemical (PEC) biosensor for ultrasensitive detection of human T-cell lymphotropic virus type I (HTLV-I) DNA. This proposed signal amplification strategy integrates λ-exonuclease (λ-Exo) aided target recycling with hybridization chain reaction (HCR) and enzyme catalysis. In the presence of target DNA (tDNA) of HTLV-I, the designed hairpin DNA (h_1DNA) hybridized with tDNA, subsequently recognized and cleaved by λ-Exo to set free tDNA. With the λ-Exo aided tDNA recycling, an increasing number of DNA fragments (output DNA, oDNA) were released from the digestion of h_1DNA. Then, triggered by the hybridization of oDNA with capture DNA (cDNA), numerous biotin-labeled hairpin DNAs (h_2DNA and h_3DNA) could be loaded onto the photoelectrode via the HCR. Finally, avidin-labeled alkaline phosphatase (avidin-ALP) could be introduced onto the electrode by specific interaction between biotin and avidin. The ALP could catalyze dephosphorylation of phospho-L-ascorbic acid trisodium salt (AAP) to generate an efficient electron donor of ascorbic acid (AA), and thereby greatly increasing the photocurrent signal. By utilizing the proposed cascade signal amplification strategy, the fabricated PEC biosensor exhibited an ultrasensitive and specific detection of HTLV-I DNA down to 11.3 aM, and it also offered an effective strategy to detect other DNAs at ultralow levels.

1. Introduction

Highly sensitive detection of DNA is of great significance for clinical diagnosis, gene therapy, mutation analysis and pathogen detection (Diao et al., 2018; Liu et al., 2009; Hänsel-Hertsch et al., 2017; Shaw et al., 2017; Wang et al., 2011). Human T-cell lymphotropic virus type I (HTLV-I) is a human retrovirus, which is associated with the clinical diagnoses of rare lymphocytic neoplasms, progressive neurodegenerative disease, and adult T-cell lymphoma/leukemia. Nevertheless, HTLV-I DNA is so fractional that more ingenious analytical strategies were necessary for detection (Kalyanaraman et al., 1982; Bhagavati et al., 1988; Poiesz et al., 1980).

Over the past decades, various techniques have been developed for sensitive detection of the specific DNA sequences, such as microarrays, colorimetric, electrochemcial, electrochemiluminescence, photoelectrochemical (PEC) biosensors, and so on (Schena et al., 1995; Teengam et al., 2017; Freeman et al., 2011; Low et al., 2017; Zhang et al., 2012; Zhao et al., 2014). Among these methods, PEC biosensor is a newly emerged yet vibrantly developing technique for biological sensing. PEC biosensors inherited the advantages of conventional electrochemical and optical methods, and offered a potential biosensing platform with high sensitivity and reduced background signal (Li et al., 2016; Zeng et al., 2014; Fan et al., 2016; Zhao et al., 2015).

In order to detect ultralow levels of DNA, the most important aspect of a sensitive PEC biosensor is to employ an excellent signal amplification strategy. To date, the signal amplification strategies for

* Corresponding authors.
E-mail addresses: iamqmshen@njupt.edu.cn (Q. Shen), jjzhu@nju.edu.cn (J.-J. Zhu).
[1] These authors contributed equally to this work.

https://doi.org/10.1016/j.bios.2018.03.023
Received 3 February 2018; Received in revised form 9 March 2018; Accepted 12 March 2018
Available online 13 March 2018
0956-5663/

ultrasensitive DNA detection have attracted more and more attention, because they can overcome the inherent limitation of target-to-signal ratio of 1:1 in the traditional hybridization assay and acquire higher sensitivity (Tao et al., 2015; Wang et al., 2015; Wu et al., 2015; Song et al., 2015). So far, a number of amplification methods have been developed, such as rolling circle amplification (RCA) (Song et al., 2015; Murakami et al., 2008; Wang et al., 2014), polymerase chain reaction (PCR) (Cheglakov et al., 2006; Du et al., 2013), hybridization chain reaction (HCR) (Choi et al., 2010; Chen et al., 2011a; Yang et al., 2015), and enzyme-assisted target recycling (Tao et al., 2015; Zuo et al., 2010; Bi et al., 2012; Ren et al., 2015). Among them, enzyme-assisted target recycling amplification has been widely adopted for the development of DNA biosensor. As one of the exonuclease, λ-exonuclease (λ-Exo) can catalyze the stepwise digestion of a 5′ phosphorylated strand in the 5′ to 3′ direction in a double-stranded DNA (dsDNA) (Kovall and Matthews, 1997). Thus, λ-Exo provides a universal platform for the target recycling amplified DNA assay. Further development in DNA signal amplification technique is the HCR technique. HCR is a complementary base paring reaction, which is triggered by a single-stranded DNA initiator and propagates a chain reaction of hybridization events to yield nicked double helices analogous to alternating copolymers, making HCR a promising strategy in signal amplification (Choi et al., 2010)

Inspired by the works discussed above, we have for the first time designed a novel ultrasensitive PEC biosensor for HTLV-I DNA detection by combining λ-Exo aided target recycling, HCR and enzyme catalysis for cascade signal amplification, as illustrated in Scheme 1. The h_1DNA consists of two regions, including the recognition region which is complementary to target DNA (tDNA) at the 5′-terminus and the output region which is partly complementary to capture DNA (cDNA). In the absence of tDNA, h_1DNA remains intact to λ-Exo because the overhang 5′-phosphorylated terminus could not be cleaved by λ-Exo. However, h_1DNA could form a dsDNA with a blunt 5′-phosphorylated terminus in the presence of tDNA (tDNA). The blunt 5′-phosphorylated terminus dsDNA could be stepwise digested by λ-Exo, and then releases the tDNA and output DNA (oDNA). The released tDNA could further take participate in the next cycles of hybridization and cleavage process (Cycle I). The introduction of HCR into the PEC DNA biosensor could further improve the detection sensitivity. The released oDNA could be captured by the cDNA on the electrode, and then open h_2DNA through hybridization, trigger the subsequent hybridization reaction by the sequential introduction of h_3DNA, and realize the downstream HCR amplification (Yang et al., 2015). The formed dsDNA chains on the electrode with the biotin-tagged h_2DNA and h_3DNA provide multiplex biotin sites, which could conjugate with avidin-alkaline phosphatase (Av-ALP) through the combination between biotin and avidin. The enzyme of ALP, which exists extensively in mammalian organisms and catalyzes the hydrolysis and transphosphorylation of diverse phosphoryl esters (Zhao et al., 2012a, 2012b), could dephosphorylate the substrate of 2-phospho-L-ascorbic acid trisodium salt (AAP) and generate the product of ascorbic acid (AA), a commonly used electron donor in PEC biosensor (Yin et al., 2015; Zhou et al., 2014). In the proposed cascade signal amplification strategy, the presence of tDNA could trigger the cycle I, releasing plenty of oDNA, and then produce more biotin sites through HCR. With the biotin sites, more Av-ALP could anchor on the DNA chains. Given the enzyme catalysis amplification of ALP, the photocurrent response could be greatly enhanced by the AA generated from AAP by ALP. The intensity of the photocurrent signal was proportional to the concentration of tDNA by this cascade signal amplification strategy. The designed PEC system exhibited excellent analytical performance, which would have promising perspective for sensitive and selective DNA detection.

2. Experimental

2.1. Materials and reagents

ITO electrodes (type JH52, ITO coating 30 ± 5 nm, sheet resistance ≤10 Ω/square) were ordered from Nanjing Zhongjingkeyi Technology Co., Ltd. (China). Graphite powder, potassium peroxydisulfate ($K_2S_2O_8$), potassium permanganate ($KMnO_4$), sulfuric acid (H_2SO_4), hydrochloric acid (HCl), phosphorus pentoxide (P_2O_5), cadmiumnitrate ($Cd(NO_3)_2{\cdot}4H_2O$, sodium sulfide(Na_2S), zinc nitrate hexahydrate ($Zn(NO_3)_2{\cdot}6H_2O$), sodium hydroxide (NaOH), and sodium chloride (NaCl) were obtained from Nanjing Chemical Reagent Co. Ltd. (China). 1-Ethyl-3-(3-dimethylaminopropyl) carbodiimide (EDC), N-hydroxysuccinimide (NHS), monoethanolamine (MEA), 3-mercaptopropionic acid (MPA), and 2-phospho-L-ascorbic acid trisodium salt (AAP) were received from Sigma-Aldrich (USA). Ascorbic acid (AA) and hydrogen peroxide (H_2O_2, 30 wt%) were purchased from Sinopharm Chemical Reagent Co., Ltd (Shanghai, China). Avidin labeled alkaline phosphatase (adivin-ALP) was purchased from Sangon Biotechnology Co. Ltd. (Shanghai, China). Lambda Exonuclease (λ-Exo) was obtained from

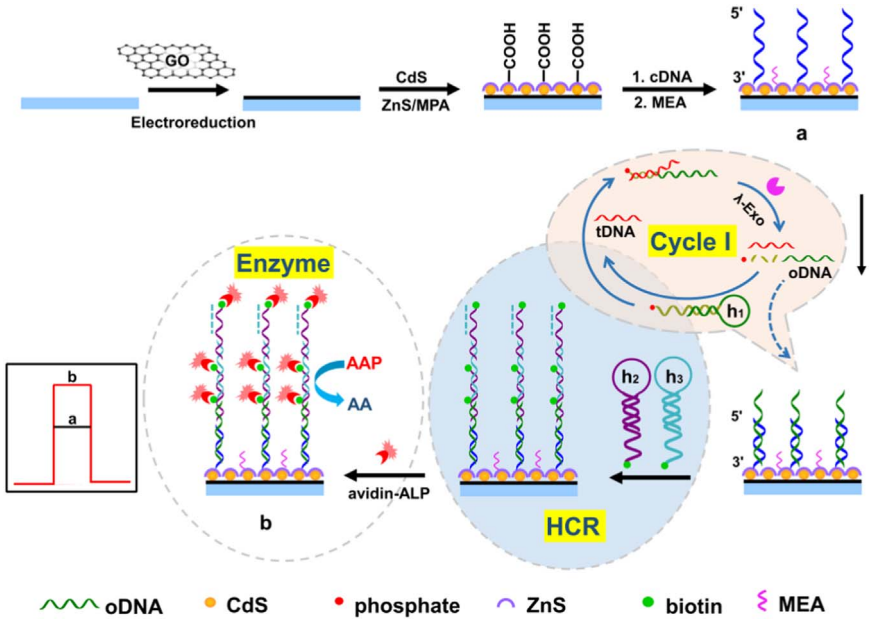

Scheme 1. Fabrication process of the PEC DNA biosensor with cascade signal amplification.

New England Biolabs. Ltd (Beijng, China). All other chemical reagents were of analytical grade and used without further purification. The solvent in each step was deionized water (DI water, 18 MΩ/cm) from a Milli-Q water purification system. Tris-HCl buffer solution (10 mM, pH 7.4) containing 10 mM NaCl and 2 mM $MgCl_2$ was used for preparation of DNA stocking solutions. 0.1 M PBS buffer solution (0.1 M NaH_2PO_4, 0.1 M Na_2HPO_4, pH 8.0) was prepared as PEC determination buffer. Avidin-ALP was diluted by 0.1 M PBS buffer (pH 7.4).

All the following DNA sequences used were ordered from Sangon Biotechnology Co. Ltd. (Shanghai, China):

cDNA, 5′-GAG GGA GTG AAA AGT-NH_2–3′;

h_1DNA, 5′-phosphorylate-TCC TCC AGG CCA TGC GCA AAA CTT TTC ACT CCC TCT TAT TTG CGC ATG GC − 3′;

tDNA (HTLV-I), 5′-GAG TAT TTG CGC ATG GCC TGG AGG A-3′;

oDNA, 5′-ACT TTT CAC TCC CTC TTA TTT GCG CAT GGC − 3′;

biotin-h_2DNA, 5′-biotin-GCG CAT GGC TTA GTT GCC ATG CGC AAA TAA − 3′;

biotin-h_3DNA, 5′-biotin-AAC TAA GCC ATG CGC TTA TTT GCG CAT GGC-3′;

one-base mismatch DNA, 5′-GAG TAT **C**TG CGC ATG GCC TGG AGG A-3′;

noncomplementary DNA, 5′-GAG TAG CGT ATA AGA CTT ATA GAC T-3′.

2.2. Apparatus

Field-emission scanning electron microscopy (FE-SEM) was carried out on a Hitachi S-4800 scanning electron microscope (Hitachi Co., Japan) equipped with EX-250 Energy-dispersive X-ray spectroscopy (EDX, HORIBA Co., Japan). Electrochemical impedance spectroscopy (EIS) was performed on an Autolab potentiostat/galvanostat (PGSTAT 30, Eco Chemie B.V., Utrecht, Netherlands) with a three-electrode system in 0.1 M KCl solution containing 2.0 mM $K_3[Fe(CN)_6]/K_4[Fe(CN)_6]$ (1:1) mixture as a redox probe, and recorded in the frequency range of 0.01 Hz-100 kHz with an amplitude of 50 mV. PEC measurements were carried out with a home-made PEC system. A 500 W Xe lamp was used as the irradiation source with the light intensity of 400 μW cm^{-2} estimated by a radiometer (Photoelectric Instrument Factory of Beijing Normal University). Photocurrent was recorded on a CHI 660D electrochemical workstation (Shanghai Chenhua Apparatus Corporation, China) with a three-electrode system: a 0.25 cm^2 modified ITO electrode as the working electrode, a Pt wire as the counter electrode, and a saturated Ag/AgCl electrode as the reference electrode.

2.3. Electrodeposition of reduced graphene oxide

First, graphene oxide (GO) solution was prepared according to a modified Hummers's method (Hummers and Offeman, 1958). For electrodeposition of reduced graphene oxide (RGO), a dispersion containing 0.8 mg/mL GO was used (Zheng et al., 2013). The cyclic voltammetric reduction was carried out on a CHI 660D electrochemical workstation using a three-electrode: the bare ITO with fixed area of 0.25 cm^2 as the working electrode, Pt wire as the counter electrode, and Ag/AgCl as the reference electrode. The scan range was between −1.3 and 0.6 V at a rate of 0.1 V/s. When the GO sheets, which directly contacted with the ITO electrode, accepted electrons to subject to electrochemical reduction, the resulted insoluble graphene sheets would directly attach onto the electrode surface (Chen et al., 2011b). After thirty cycles of scan, the working electrode was rinsed with DI water.

2.4. Preparation of the ITO/RGO/CdS/ZnS PEC electrode

After electrodeposition of RGO, the modified ITO electrode was then deposited with CdS nanocrystals by successive ionic layer adsorption and reaction (SILAR) technique (Li et al., 2012). Specifically, the ITO/RGO electrode was initially immerged into 0.1 M $Cd(NO_3)_2$ methanol solution for 1 min and washed with methanol, then followed by immerging into 0.1 M Na_2S methanol/water mixture (1:1, v/v) for 1 min, and again washed with methanol. This SILAR cycle was repeated for five times until desired ITO/RGO/CdS electrode was obtained. Subsequently, the CdS nanocrystals modified electrode was deposited with ZnS nanocrystals also by the SILAR method. The electrode was alternatively immerged in 0.1 M $Zn(NO_3)_2$ methanol solution and 0.1 M Na_2S methanol/water mixture (1:1, v/v) for 1 min of each with intermediate methanol washing. When the cycle number for ZnS layer was three, the obtained ITO/RGO/CdS/ZnS PEC electrode was employed to immobilize DNA sequences in the next process of the DNA biosensor fabrication.

2.5. λ-Exo aided tDNA recycling

The λ-Exo reaction buffer consisted of 67 mM glycine-KOH (pH 9.4), 2.5 mM $MgCl_2$, and 0.01% (v/v) Triton X-100. First, 40 μL of solution containing 20 μL of 1 μM h_1DNA and different concentrations of tDNA was incubated for 2 h at 37 °C. Then, 5 μL of λ-Exo (2 U/μL) and 5 μL of λ-Exo buffer were added in the mixture solution mentioned above, and kept at 37 °C for 60 min followed by terminating the λ-Exo reaction with 2 μL of 0.5 M EDTA solution. The resulting reaction solution containing oDNA was set aside, waiting for use next.

2.6. Fabrication of PEC DNA biosensor

First, the ITO/RGO/CdS/ZnS PEC electrode was immersed into 0.5 mL of 3 mM MPA solution for 5 h at 4 °C (Shan et al., 2009). After the electrode was rinsed with Tris-HCl buffer (10 mM, pH = 7.4) to remove unbound MPA, the carboxy groups of MPA modified on the electrodes were activated by dropping 25 μL of 10 mM EDC and 20 mM NHS solution on the electrode surface for 50 min at room temperature. Then, 20 μL of 1 μM cDNA solution was dropped onto the electrode and maintained at 4 °C for 12 h. The cDNA sequences were immobilized on the electrode by classic EDC coupling reaction between carboxy groups of MPA and the amino group of cDNA. Then, the electrode was washed with Tris-HCl buffer, blocked with 20 μL of 1 mM MEA at room temperature for 1 h and washed with Tris-HCl buffer again. Subsequently, the electrode was incubated in the solution of oDNA coming from λ-Exo aided tDNA recycling for 60 min at room temperature to immobilize oDNA on the electrode through the DNA hybridization between cDNA and oDNA. After being washed with Tris-HCl buffer, the electrode was immersed in the Tris-HCl buffer solution containing 1 μM biotin-h_2DNA and 1 μM biotin-h_3DNA at room temperature for 2 h to carry out the hybridization chain reaction. Afterwards, the electrode was rinsed with Tris-HCl buffer and incubated with 20 μL of avidin-ALP (2 μg/mL) at 37 °C for 30 min. After being rinsed with Tris-HCl buffer, the electrode was ready for PEC determination.

2.7. PEC measurement

PEC tests were operated at room temperature in PBS buffer (0.1 M, pH 8.0) containing 10 mM AAP, which acted as a substrate of ALP to produce an efficient electron donor of AA. The electrolyte was deaerated with pure nitrogen for 10 min before PEC test. Xenon lamp was used as irradiation source with a wavelength range of 0.4–2.5 μm, which was turned on and off every 10 s. The electrochemical method was current-time curve with 0.0 V applied voltage.

3. Results and discussion

3.1. SEM characterization of the ITO/RGO/CdS/ZnS electrode

The surface morphologies of the ITO/RGO/CdS/ZnS electrodes during the fabrication process were characterized by SEM. Fig. 1A-D

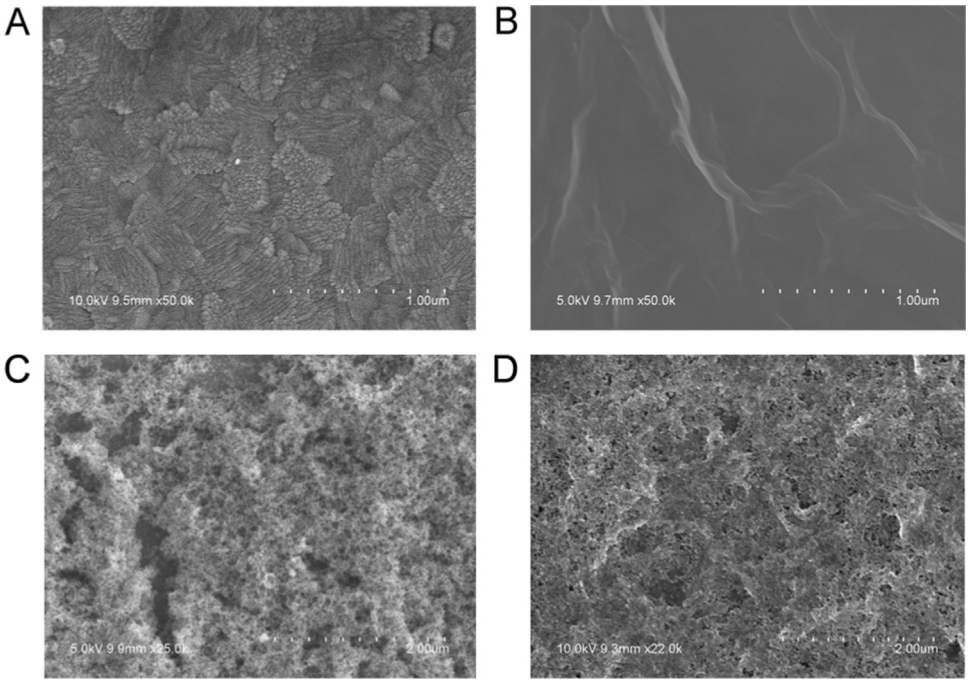

Fig. 1. SEM images of the (A) bare ITO, (B) ITO/RGO, (C) ITO/RGO/CdS, and (D) ITO/RGO/CdS/ZnS electrodes.

shows SEM images of the bare ITO, ITO/RGO, ITO/RGO/CdS, and ITO/RGO/CdS/ZnS electrode surfaces in order. The bare ITO was fully carpeted with plenty of indium tin oxide nanoclusters (Fig. 1A). After RGO electrodeposition, RGO nanosheets with abundant wrinkles were adhered on the electrode (Fig. 1B), which could offer a larger specific area to deposit more photoactive nanomaterials. After CdS modification, a large number of nanocrystals (with the diameter of 4–10 nm) as well as pores could be observed (Fig. 1C). After ZnS modification, the size of the nanocrystals on electrode surface increased to 7–12 nm, which confirmed that ZnS nanocrystals had been successfully coated on the surface of CdS nanocrystals (Fig. 1D). Besides, the EDX spectroscopy of the ITO/RGO/CdS/ZnS electrode during the fabrication process was also characterized, as shown in Fig. S1, which further confirmed successful formation of the electrode.

3.2. PEC property of the ITO/RGO/CdS/ZnS electrode

Graphene with two-dimensional morphology has large surface area and superior electrical conductivity, and it has been extensively considered as a promising candidate for electron-acceptor and electron transport matrices. CdS is a well-known semiconductor with a narrow band gap (~2.4 eV) used in solar cells, since it can effectively absorb visible light and generate electron-hole pairs, resulting in high PEC activity (Shen et al., 2011). ZnS with wide band gap (~3.8 eV) was commonly used as a passivation layer for photoelectrode. It not only prohibited the formation of surface defects on CdS, but also blocked the charge recombination of the narrow band-gap of CdS (Santra and Kamat, 2012). The conduction band (CB) and valance band (CB) levels of the ITO/RGO/CdS/ZnS electrode were shown in panel A of Fig. S2. The cascade energy level of the ITO/RGO/CdS/ZnS electrode boosted electron transfer between them. In order to examine the PEC property of the ITO/RGO/CdS/ZnS electrode, the photocurrent responses of the ITO/RGO/CdS/ZnS electrode during each step of fabrication were tested. As illustrated in panel B of Fig. S2, after RGO electrodeposition on the ITO electrode, a very small photocurrent could be observed (curve a), since the RGO does not have PEC property. After CdS modification, the photocurrent intensity increased evidently (curve b). It was because RGO offered large surface area for CdS deposition and the RGO/CdS nanocomposites could widen the light absorption range, facilitate the spatial separation of photogenerated electron-hole pairs and accelerate electron transfer. The photocurrent intensity further increased after ZnS modification (curve c), which was because ZnS could block the charge recombination and meanwhile act as a passivation shell to reduce surface defect states of CdS.

3.3. PEC characterization of the DNA biosensor

The fabrication process of the designed PEC DNA biosensor was characterized by photocurrent response, as shown in Fig. 2A. The ITO/RGO/CdS/ZnS PEC electrode exhibited an obvious photocurrent

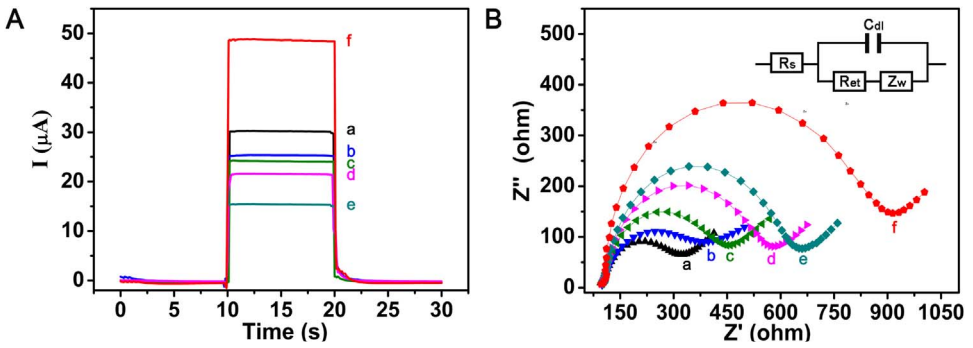

Fig. 2. (A) Photocurrent responses and (B) EIS of (a) the ITO/RGO/CdS/ZnS electrode, (b) cDNA modification, (c) MEA immobilization, (d) oDNA hybridization with cDNA by λ-Exo aided target recycling, (e) HCR trigged by oDNA, and (f) avidin-ALP immobilization. Inset of panel B: the applied electrical equivalent circuit; R_{et}, Z_w, C_{dl}, and R_s denote electron transfer resistance, Warburg impedance, the double-layer capacitance, and ohmic resistance of the electrolyte, respectively.

response (curve a, $I = 30.20$ μA). After cDNA and MEA immobilization, the photocurrent intensity decreased moderately (curve b, $I = 25.34$ μA; curve c, $I = 24.11$ μA), which could be ascribed to the relatively weak charge transfer of short DNA sequences as well as MEA molecules. When the cDNA hybridized with oDNA, which produced by λ-Exo aided tDNA recycling, the decrease of photocurrent intensity could be attributed to the increase of steric hindrance and the poor electron-transfer efficiency of the DNA doule-helix (curve d, $I = 21.54$ μA). After HCR was triggered by oDNA, the photocurrent intensity further decreased due to the formation of double-strand DNA polymers composed of biotin-h_2DNA and biotin-h_3DNA (curve e, $I = 15.39$ μA). As expected, the electrode showed an evidently increased photocurrent intensity after avidin-ALP immobilization through the specific interaction between avidin and biotin (curve f, $I = 48.64$ μA). The increase of photocurrent could be attributed to the produced electron donor of AA by ALP catalysis, which could capture photo-generated holes and improve photocurrent signal effectively. Thus, the trends in photocurrent changes confirmed the successful construction of the PEC DNA biosensor.

3.4. EIS characterization of the DNA biosensor

The fabrication of the DNA biosensor was also characterized by electrochemical impedance spectroscopy (EIS). As shown in Fig. 2B, each impedance spectrum was composed of a semicircle at higher frequencies related to the electron-transfer resistance and a linear part at lower frequencies associated with the diffusion process. Thereinto, the semicircle diameter equals the electron-transfer resistance (R_{et}), which represents the restricted diffusion of the redox probe accessing the interface layer. The inset of Fig. 2B displays the applied electrical equivalent circuit fitting to the impedance spectra. For ITO/RGO/CdS/ZnS PEC electrode, the impedance spectrum exhibited a relatively small semicircle corresponding to a small R_{et} (curve a). After cDNA and MEA immobilization, the gradual increase of R_{et} was observed due to the low conductivity of DNA sequence and MEA molecules (curves b and c). After the hybridization between cDNA and oDNA produced by λ-Exo aided tDNA recycling, and then the HCR trigged by oDNA, the R_{et} also increased gradually (curve d and e) due to poor conductivity of the double-strand oligonucleotides. As the avidin-ALP was bound on the electrode via specific interaction between avidin and biotin, the evident increase in R_{et} was observed (curve f). It was because the modified enzyme of ALP formed a barrier layer and prevented the redox probe from accessing the electrode surface. Therefore, the EIS results also suggested the successful fabrication of the DNA biosensor.

3.5. Optimal conditions of the ITO/RGO/CdS/ZnS PEC electrode

Fig. 3A shows photocurrent intensity of the ITO/RGO/CdS/ZnS electrode electrodeposited with different cycles of RGO, with five layers of CdS fixed. It could be seen the photocurrent intensity gradually increased with the cycle number increasing to thirty. After that, the photocurrent decreased, since excessive RGO would have side effect on the excitation of subsequently modified CdS layers (Zhao et al., 2012a, 2012b). Fig. 3B shows photocurrent intensity of the ITO/RGO/CdS electrode deposited with different layers of CdS, with thirty cycles of RGO fixed. With the increase of CdS layer, more CdS nanoparticles led to higher light absorption and enhanced photocurrent intensity. The ITO/RGO/CdS electrode with five CdS layers owned the maximum photocurrent intensity. After further increase in CdS layer, the excessive CdS would form more surface recombination centers, which increased the diffusion resistance for electron motion, and therefore, resulting in the gradual decrease of photocurrent intensity (Vogel et al., 1994). Fig. 3C shows photocurrent intensity of the ITO/RGO/CdS/ZnS electrode deposited with different layers of ZnS, with thirty cycles of RGO as well as five layers of CdS fixed. It could be seen that three layers of ZnS deposition exhibited the maximum photocurrent intensity, and the explanation was similar to the CdS deposition. Accordingly, the ITO/RGO/CdS/ZnS electrode deposited with thirty cycles of RGO, five layers of CdS, and three layers of ZnS was chosen as the optimal condition to the fabrication of the PEC DNA biosensor.

3.6. Optimal conditions of the DNA biosensor

The enzyme of λ-Exo was used to digest the hybridized h_1DNA and set free tDNA for recycling. As a result, the incubation time of λ-Exo showed an obvious effect on the photocurrent response. Fig. 4A displays photocurrent intensity of the biosensor at different incubation time points in 20 μL of 1 μM tDNA and 2 U λ-Exo. The gradual increase of photocurrent intensity could be observed with the increment of the incubation time and then got a flat at 60 min, implying achievement of the λ-Exo aided tDNA recycling. Thus, 60 min was used as the optimal incubation time. The enzyme of ALP could dephosphorylate AAP to produce AA, an effective electron donor to increase the intensity of photocurrent. As the generation of AA was a time-based process, the time of ALP catalysis had an evident influence on the performance of the DNA biosensor (Shen et al., 2015). The longer catalysis time was, the more AA could be generated to capture the photo-generated holes and the better photocurrent intensity was. Fig. 4B shows the influence of ALP catalysis time on photocurrent response of the biosensor. The photocurrent intensity ascended with the increase of catalysis time to 30 min. While the catalysis time was postponed to 40 min, the intensity showed a stable trend. Thus, 30 min of ALP catalysis was the appropriate experiment condition for the DNA biosensor.

3.7. PEC detection of the tDNA

The photocurrent intensity of PEC DNA biosensor was found to be directly related the modified amount of the ALP, which was indirectly associated with the tDNA concentration. Fig. 5A shows the photocurrent responses of the DNA biosensor after being incubated with

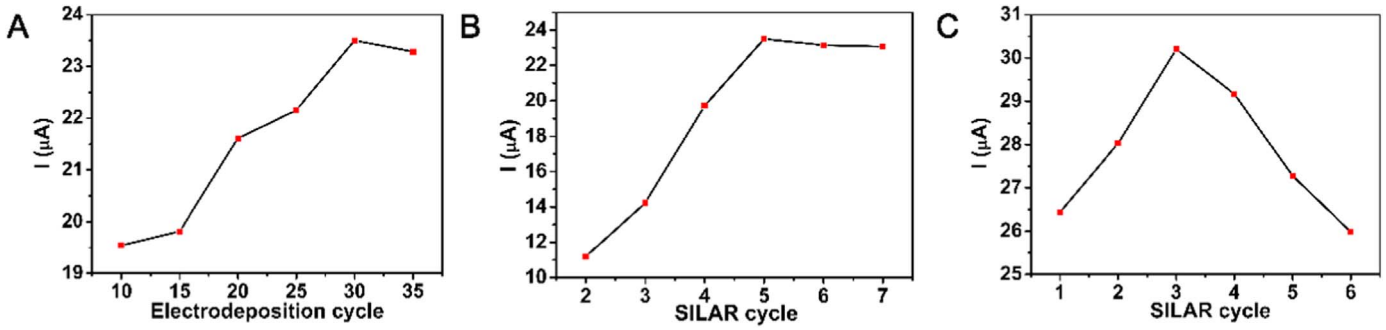

Fig. 3. Influences of (A) the cycles of RGO nanosheets, (B) the layers of CdS nanocrystals, and (C) the cycles of ZnS nanocrystals on photocurrent response of the ITO/RGO/CdS/ZnS electrode.

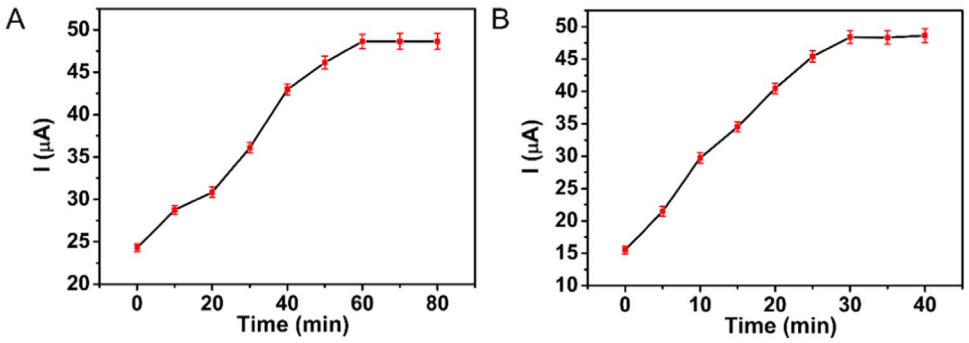

Fig. 4. Evaluation of the photocurrent responses to (A) different λ-Exo incubation time and (B) different ALP catalysis time of the DNA biosensor.

different concentrations of tDNA. Along with the increase in the concentration of tDNA, more amount of ALP would bind on the electrode and generate plenty of AA electron donors, and therefore, the photocurrent signal gradually enhanced. As shown in Fig. 5B, the intensity of photocurrent was proportional to the logarithm of the tDNA concentration in the linear range from 50 aM to 100 pM. The linear regression equation was $I = 40.65 + 3.0376 \log C$ (pM), with correlation coefficient of 0.9985. The detection limit (S/N = 3) was calculated to be 11.3 aM. The designed DNA biosensor with cascade signal amplification presented a much lower detection limit as well as a wider linear range than many previously reported results for HTLV-I DNA detection (Norouzi et al., 2017; Yang et al., 2010, 2011; Zhang et al., 2009).

3.8. Selectivity, reproducibility, and stability of the PEC biosensor

In order to verify the selectivity of the designed DNA biosensor, the photocurrent signals to different preset hybridizations including tDNA, one-base mismatch, and noncomplementary DNA sequences were investigated, where the concentration of each DNA sequence was kept at 10 pM. As shown in Fig. S3, the photocurrent response of HTLV-I DNA was much higher than those of mismatch DNA or control sample solution, which demonstrated that the designed biosensor could effectively discriminate different DNA sequences. All these comparing results proved that the photocurrent signal was specifically enhanced by the presence of tDNA and was further amplified by cascade signal amplification strategy. Thus, it was demonstrated that the designed PEC DNA biosensor had a satisfying selectivity.

The reproducibility of the PEC DNA biosensor was assessed by inter-assay relative standard deviation (RSD) by analyzing five biosensors prepared separately. After the cDNA modified PEC electrode was incubated with tDNA and meanwhile underwent the cascade signal amplification by λ-Exo assisted target recycling, HCR, and ALP catalysis, the photocurrent signals of the biosensors offered the RSDs of 3.4% and 3.9% toward 10 fM and 100 fM tDNA detection, which indicated an acceptable reproducibility of this DNA biosensor.

The stability of the PEC DNA biosensor was evaluated by testing the photocurrent change of the sensing electrode before and after storage. Two groups of the biosensor were prepared under the same conditions and each group was composed of five electrodes. The photocurrent responses of the first electrodes group were tested as preparation, and their average value served as the original value. After being stored at 4 °C for one month, the average photocurrent response of the second electrodes group maintained 95.6% of its original value, indicating good storage stability.

4. Conclusion

In summary, a promising enhanced PEC biosensor for ultrasensitive detection of HTLV-I DNA was developed based on cascade signal amplification. The good performance of the biosensor was ascribed to the high sensitivity of the PEC technique and the cascade signal amplification by λ-Exo assisted target recycling, HCR and multi-ALP enzyme labels. By employing the cascade signal amplification, the PEC biosensor could offer a low detection limit with a wide detection range of HTLV-I DNA, which was more sensitive than that previously reported results. Furthermore, the inherent selectivity of h_1DNA and λ-Exo endow the biosensor with high differentiation of similar DNA. Featured by its high sensitivity and specificity, the cascade signal amplification strategy may offer a novel platform to detect DNA with trace levels and give an effective assessment to early diagnosis of diseases.

Acknowledgments

We appreciate the financial support from the National Natural Science Foundation of China (21575069 and 21603099), Education Ministry of China (No. IRT1148), Synergetic Innovation Center for Organic Electronics and Information Displays and a project funded by Priority Academic Program Development of the Jiangsu Higher Education Institutions.

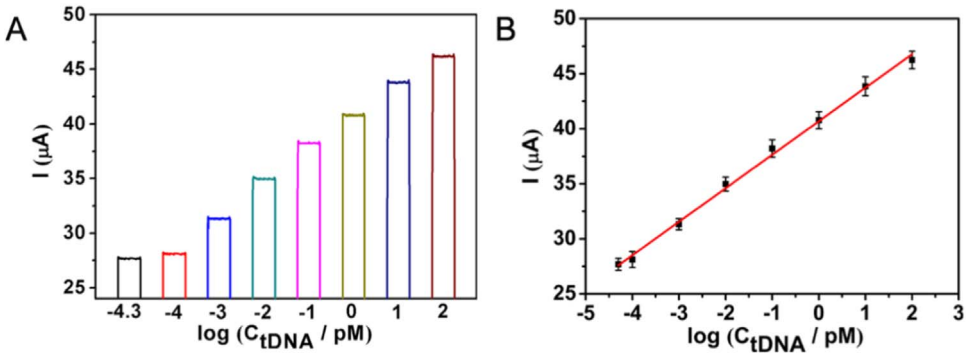

Fig. 5. (A) Photocurrent response and (B) calibration curve of the PEC biosensor to different concentrations of HTLV-I DNA. The error bars represented standard deviations of five replicate measurements.

Appendix A. Supporting information

Supplementary data associated with this article can be found in the online version at http://dx.doi.org/10.1016/j.bios.2018.03.023.

References

Bi, S., Li, L., Cui, Y.Y., 2012. Chem. Commun. 48, 1018–1020.
Bhagavati, S., Ehrlich, G., Kula, R.W., Kwok, S., Sninsky, J., Udani, V., Poiesz, B.J., 1988. N. Engl. J. Med. 318, 1141–1147.
Cheglakov, Z., Weizmann, Y., Beissenhirtz, M.K., Willner, I., 2006. Chem. Commun. 3205–3207.
Diao, W., Tang, M., Ding, S., Li, J., Chen, X.M., Mo, W.B., Yan, F., Ma, X.Y., Yan, Y. R, H.M., 2018. Biosens. Bioelectron. 100, 228–234.
Du, Y.Q., Gao, P.F., Wang, W., Wang, T.T., Chang, Y., Wang, J., Huang, C.Z., 2013. Analyst 138, 5745–5750.
Chen, X., Lin, Y.H., Li, J., Lin, L.S., Chen, G.N., Yang, H.H., 2011a. Chem. Commun. 47, 12116–12118.
Chen, L., Tang, Y., Wang, K., Liu, C., Luo, S., 2011b. Electrochem. Commun. 13, 133–137.
Choi, H.M., Chang, J.Y., Trinh, L.A., Padilla, J.E., Fraser, S.E., Pierce, N.A., 2010. Nat. Biotechnol. 28, 1208–1212.
Fan, G.C., Zhu, H., Du, D., Zhang, J.R., Zhu, J.J., Lin, Y.H., 2016. Anal. Chem. 88, 3392–3399.
Freeman, R., Liu, X.Q., Willner, I., 2011. J. Am. Chem. Soc. 133, 11597–11604.
Hänsel-Hertsch, R., Di Antonio, M., Balasubramanian, S., 2017. Nat. Rev. Mol. Cell Bio. 18, 279–284.
Hummers Jr, W.S., Offeman, R.E., 1958. J. Am. Chem. Soc. 80 (1339 – 1339).
Kalyanaraman, V.S., Sarngadharan, M.G., Robert-Guroff, M., Miyoshi, I., Blayney, D., Golde, D., Gallo, R.C., 1982. Science 571–573.
Kovall, R., Matthews, B.W., 1997. Science 277, 1824–1827.
Li, L., Zhang, Y., Zhang, L.N., Ge, S.G., Liu, H.Y., Ren, N., Yan, M., Yu, J.H., 2016. Anal. Chem. 88, 5369–5377.
Li, T.L., Lee, Y.L., Teng, H.S., 2012. Energy Environ. Sci. 5, 5315–5324.
Liu, J., Cao, Z.H., Lu, Y., 2009. Chem. Rev. 109, 1948–1998.
Low, K.F., Zain, Z.M., Yean, C.Y., 2017. Biosens. Bioelectron. 87, 256–263.
Murakami, T., Sumaoka, J., Komiyama, M., 2008. Nucleic Acids Res. 37, e19.
Norouzi, M., Ghobadi, M.Z., Golmimi, M., Mozhgani, S.H., Ghourchian, H., Rezaee, S.A., 2017. Anal. Lett. 50, 2402–2411.
Poiesz, B.J., Ruscetti, F.W., Gazdar, A.F., Bunn, P.A., Minna, J.D., Gallo, R.C., 1980. Proceedings Natl. Acad. Sci. (U.S.A.) 77, pp. 7415 – 7419.
Ren, W., Gao, Z.F., Li, N.B., Luo, H.Q., 2015. Biosens. Bioelectron. 63, 153–158.
Santra, P.K., Kamat, P.V., 2012. J. Am. Chem. Soc. 2012 (134), 2508–2511.
Schena, M., Shalon, D., Davis, R.W., Brown, P.K., 1995. Science 467–470 (New York, N. Y.).
Shan, Y., Xu, J.J., Chen, H.Y., 2009. Chem. Commun. 905–907.
Shaw, J.A., Guttery, D.S., Hills, A., Fernandez-Garcia, D., Page, K., Rosales, B.M., Goddard, K.S., Hastings, R.K., Luo, J.L., Ogle, O., Woodley, L., Ali, S., Stebbing, J., Coombes, R.C., 2017. Clin. Cancer Res. 23, 88–96.
Shen, Q.M., Han, L., Fan, G., Zhang, J.R., Jiang, L.P., Zhu, J.J., 2015. Anal. Chem. 87, 4949–4956.
Shen, Q.M., Zhao, X.M., Zhou, S.W., Hou, W.H., Zhu, J.J., 2011. J. Phys. Chem. C. 115, 17958–17964.
Song, W., Zhang, Q., Sun, W., 2015. Chem. Commun. 51, 2392–2395.
Tao, C.Y., Yan, Y.R., Xiang, H., Zhu, D., Cheng, W., Ju, H.X., Ding, S.J., 2015. Chem. Commun. 51, 4220–4222.
Teengam, P., Siangproh, W., Tuantranont, A., Vilaivan, T., Chailapakul, O., Henry, C.S., 2017. Anal. Chem. 89, 5428–5435.
Vogel, R., Hoyer, P., Weller, H., 1994. J. Phys. Chem. 98, 3183–3188.
Wang, L., Deng, R., Li, J., 2015. Chem. Sci. 6, 6777–6782.
Wang, F., Elbaz, J., Orbach, R., Magen, N., Willner, I., 2011. J. Am. Chem. Soc. 133, 17149–17151.
Wang, Q., Yang, C.Y., Xiang, Y., Yuan, R., Chai, Y.Q., 2014. Biosens. Bioelectron. 55, 266–271.
Wu, C.C., Cansiz, S., Zhang, L.Q., Teng, I.T., Qiu, L.P., Li, J., Liu, Y., Zhou, C.S., Hu, R., Zhang, T., Cui, C., Cui, L., Tan, W.H., 2015. J. Am. Chem. Soc. 137, 4900–4903.
Yang, C.Y., Shi, K., Dou, B.T., Xiang, Y., Chai, Y.Q., Yuan, R., 2015. ACS Appl. Mater. Interfaces 7, 1188–1193.
Yang, X., Du, Y., Li, D., Lv, Z.Z., Wang, E.K., 2011. Chem. Comm. 47, 10581–10583.
Yang, X., Sun, X.P., Lv, Z.Z., Guo, W.W., Du, Y., Wang, E.K., 2010. Chem. Comm. 46, 8818–8820.
Yin, H.S., Sun, B., Dong, L.F., Li, B.C., Zhou, Y.L., Ai, S.Y., 2015. Biosens. Bioelectron. 64, 462–468.
Zeng, X.X., Tu, W.W., Li, J., Bao, J.C., Dai, Z.H., 2014. ACS Appl. Mater. Interfaces 6, 16197–16203.
Zhang, D.C., Yan, Y.R., Li, Q., Yu, T.X., Cheng, W., Wang, L., Ju, H.X., Ding, S.J., 2012. J. Biotechnol. 160, 123–128.
Zhang, X.R., Su, H.R., Bi, S., Li, S.G., Zhang, S.S., 2009. Biosens. Bioelectron. 24, 2730–2734.
Zhao, W.W., Ma, Z.Y., Yan, D.Y., Xu, J.J., Chen, H.Y., 2012a. Anal. Chem. 84, 10518–10521.
Zhao, W.W., Xu, J.J., Chen, H.Y., 2014. Chem. Rev. 114, 7421–7441.
Zhao, W.W., Xu, J.J., Chen, H.Y., 2015. Chem. Soc. Rev. 44, 729–741.
Zhao, X., Zhou, S., Jiang, L.P., Hou, W., Shen, Q., Zhu, J.J., 2012b. Chem. Eur. J. 2012 (18), 4974–4981.
Zheng, T.T., Tan, T.T., Zhang, Q.F., Fu, J.J., Wu, J.J., Zhang, K., Zhu, J.J., Wang, H., 2013. Nanoscale 5, 10360–10368.
Zhou, S.W., Kong, Y., Shen, Q.M., Ren, X.L., Zhang, J.R., Zhu, J.J., 2014. Anal. Chem. 86, 11680–11689.
Zuo, X.L., Xia, F., Xiao, Y., Plaxco, K.W., 2010. J. Am. Chem. Soc. 132, 1816–1818.